LA-UR -86-3796

Los Alamos National Laboratory is operated by the University of California for the United States Department of Energy under contract W-7405-ENG-36.

LA-UR--86-3796

DE87 002915

TITLE: A REVIEW OF WHAT NUMERICAL SIMULATIONS TELL US ABOUT THE INTERNAL ROTATION OF THE SUN

AUTHOR(S): Gary A. Glatzmaier, ESS-5

SUBMITTED TO: Proceedings of the National Solar Observatory 1986 Symposium
Sun Spot, New Mexico
August 1986

DISCLAIMER

Los Alamos Los Alamos National Laboratory
Los Alamos, New Mexico 87545

A REVIEW OF WHAT NUMERICAL SIMULATIONS TELL US ABOUT THE INTERNAL ROTATION OF THE SUN

Gary A. Glatzmaier
ESS-5 MS F665
Los Alamos National Laboratory
Los Alamos, NM 87545
USA

ABSTRACT. The simulated solar differential rotation from two independent numerical modeling efforts agree with each other and with present solar observations. The models solve the nonlinear, three-dimensional, time-dependent, anelastic equations of motion for thermal convection in a stratified, rotating, spherical shell. The simulated angular velocity in the convection zone is constant on cylinders coaxial with the rotation axis, maximum at the equator and decreasing with depth. The latitudinal variation of this angular velocity at the surface is in agreement with Doppler measurements of the solar surface rotation rate. The radial variation through the convection zone is consistent with the analysis of the rotational frequency splitting of solar oscillations.

1. INTRODUCTION

Two numerical models of global convection in the sun will be discussed. One was developed by Peter Gilman (Gilman & Miller 1986) based on an earlier Boussinesq model (Gilman 1977); the other was developed by the author (Glatzmaier 1984). Except for construction of the anelastic equations in spherical coordinates (Gilman & Glatzmaier 1981), these models have been developed completely independently. They represent an approach to the theoretical investigation of the internal dynamics of the sun that maximizes the role of physics and minimizes the role of parameterization. This approach, although expensive in terms of both comupter resources and code development, is becoming more feasible with the continued improvement and availability of supercomputers.

After briefly describing the two models, I will discuss some properties of the numerical solutions and compare them to solar observations. Particular emphasis will be placed on the simulated differential rotation. I will finish with a discussion of model validation.

2. DESCRIPTION OF MODELS

These two models are very similar in many ways and very different in many others. Both models solve the nonlinear, three-dimensional, time-dependent, anelastic equations of motion for thermal convection of a density-stratified perfect gas in a rotating, spherical shell. These models also serve as self-consistent dynamo models when the magnetohydrodynamic equations are solved (Gilman & Miller 1981; Gilman 1983;

Glatzmaier 1984, 1985a,b).

The anelastic approximation (Gough 1969; Gilman and Glatzmaier 1981) is based on the assumption that the convective velocities are small compared to the local sound speed and that the resulting thermodynamic perturbations are small compared to the respective thermodynamic variables. These are good approximations for the deep solar convection zone. The anelastic gas is compressible on a convective time scale, but not on an acoustic time scale. In other words, the sound speed is assumed to be infinite. The anelastic approximation has the advantage of being able to account for large stratifications in the thermodynamic variables, which is not accounted for in the Boussinesq approximation, while not requiring a very small time step which is needed in fully compressible calculations to resolve sound waves.

Both models have been designed as numerical analogs of global convection in the sun by constraining the mass, luminosity, average rotation rate, and radius to solar values. In practice, only the solar convection zone is simulated and only out to 90% of the solar radius (93% in Glatzmaier's model) due to large numerical resolution requirements near the solar surface resulting from the small pressure scale-heights there. Stress-free, impermeable, constant heat flux boundary conditions are applied at the inner and outer spherical boundaries.

The basic reference states of the two models differ somewhat. Gilman's model convection zone spans five pressure scale-heights and is superadiabatic everywhere. Glatzmaier's model spans seven pressure scale-heights and is superadiabatic in the upper two thirds (in radius) of the shell and subadiabatic in the lower third. This latter case is designed to simulate convective penetration into a stable region below. However, due to the large additional numerical resolution that would be required to simulate a stratification like that in a standard solar model, the modeled stable region is only slightly subadiabatic.

The present supercomputers have made three-dimensional numerical simulations possible today; however, the affordable numerical resolution in space and time is still very far from what would be required to resolve the many orders of magnitude in scale that exist in solar convection. Consequently, these global models resolve as many of the large scales as possible and parameterize, via eddy diffusion, the transport of momentum and heat by all the smaller unresolved scales. This parameterization is the weakest part of the models. However, the more modes that are resolved, i.e., the higher the numerical resolution, the less significant the unresolved modes should be in determining the structure and time-dependence of the resolved modes.

The parameterized viscous and thermal diffusivities in these models are usually specified time-independent functions of radius (either constant in radius or increasing with radius). Glatzmaier has also employed a time-dependent eddy diffusivity that depends on the local shear of the large-scale resolved velocity. In addition, the ratio of the viscous to thermal diffusivity is specified. Gilman typically sets this ratio to one; Glatzmaier usually makes it somewhat less than one. The effects of different eddy diffusivity parameterizations will be discussed in section 4.2.

The most significant difference between the two models is the numerical solution technique. In Gilman's model, Fourier expansions describe the longitudinal dependence of the functions while a finite difference scheme on a staggered grid is used in radius and latitude. The spatial resolution is 90 grid points in latitude times 20 grid points in radius times 24 longitudinal wave numbers. The equations are integrated in time via an explicit leap-frog scheme with 1.36 hour time steps.

In Glatzmaier's model, the longitudinal and latitudinal dependence of the functions is described by spherical harmonic expansions while the radial dependence is described by Chebyshev polynomial expansions. A spectral transform method is employed which computes all spatial derivatives analytically in spectral space and all nonlinear terms in

physical space each time step. The spatial resolution is 32 grid points in latitude times 33 grid points in radius times 64 grid points in longitude. Semi-implicit time-integration treats the nonlinear terms with an explicit Adams-Bashforth scheme and the linear terms with an implicit Crank-Nicolson scheme. A three hour time step is used.

3. NUMERICAL RESULTS

Although the numerical techniques employed in these models are quite different, the numerical solutions are qualitatively the same. Several properties of the numerical solutions from both models will now be described.

3.1. Time and wave number dependence

The initial conditions, for both models, are small random entropy perturbations with zero velocity relative to the rotating frame of reference. Due to buoyancy forces resulting from the entropy perturbations in the superadiabatic environment, convective velocities quickly develop and organize into large scale cellular convection. The amplitude of this motion grows exponentially in time, due to the supercritical linear terms in the equations of motion, until the nonlinear terms become large enough to terminate the growth. Kinetic energy increases at the expense of the entropy stratification which becomes less superadiabatic.

A time trace of kinetic energy is displayed in Figure 1 for one of Gilman's solutions. (Glatzmaier's model produces very similar kinetic energy traces.) The energy in the differential rotation (the axisymmetric part of the longitudinal component of velocity relative to the rotating frame of reference) is plotted separately. The nonaxisymmetric convective structure organizes within about two rotation periods (~1000 time steps); however, the differential rotation amplitude and structure, which is maintained primarily by the nonlinear interaction of the nonaxisymmetric convective modes, requires about 30 to 40 rotation periods to become fully established.

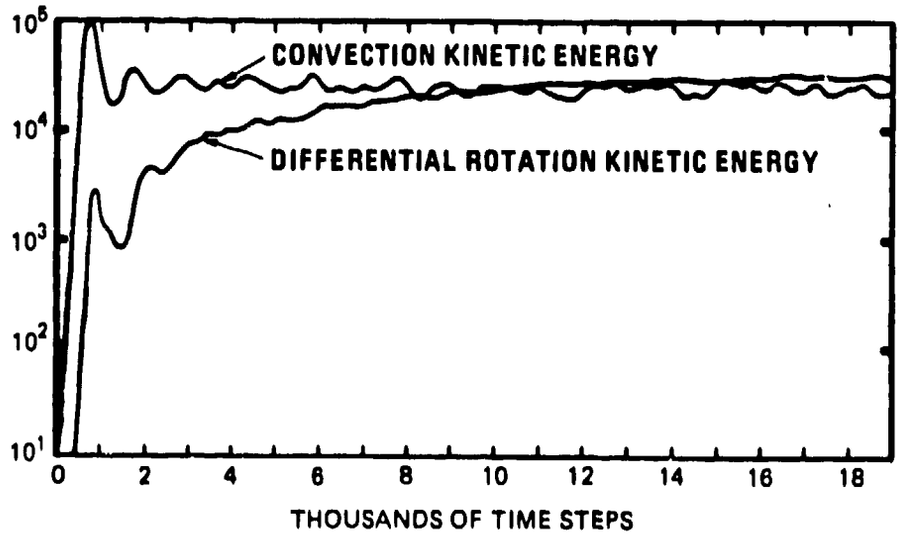

Figure 1. Kinetic energy of convection and differential rotation as a function of time (one time step = 1.36 hours; Gilman & Miller 1986). A dimensionless energy scale is used.

Energy spectra illustrate the large number of degrees of freedom associated with these three-dimensional simulations. The kinetic energy and thermal energy (entropy variance) integrated in radius and latitude are plotted as functions of longitudinal wave number *(m)* in Figure 2 for one of Glatzmaier's fully developed solutions at on instant in time. (A kinetic energy spectra, averaged in time, is illustrated in Figure 2 of Gilman & Miller 1986.) The peak in the axisymmetric *(m=0)* velocity mode is mainly due to the induced differential rotation; whereas, the peak in the axisymmetric entropy perturbation mode represents the tendency for convection to decrease the entropy stratification. In addition, broad peaks exist around *m=10* reflecting the most unstable, nonaxisymmetric, convective modes.

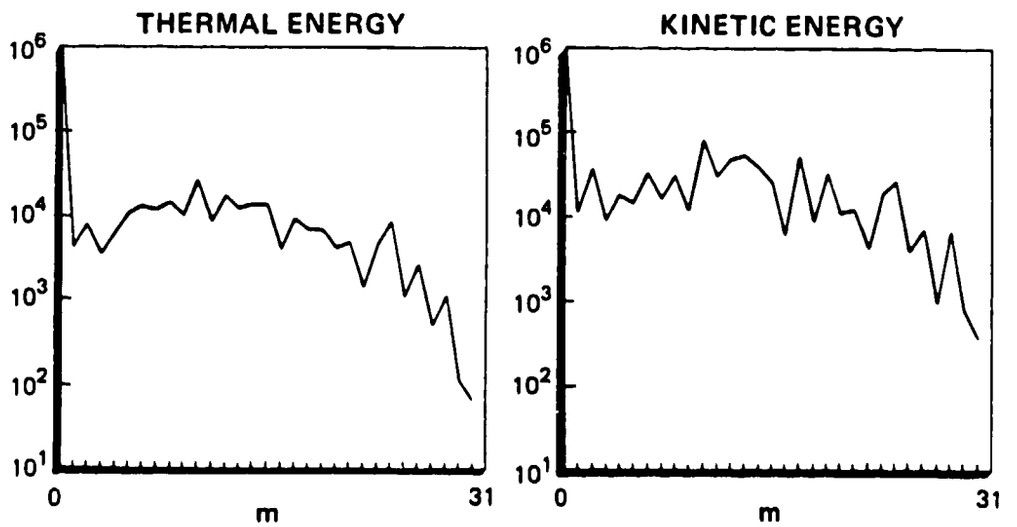

Figure 2. Thermal energy (variance of entropy perturbation) and kinetic energy integrated in radius and latitude and plotted as functions of longitudinal wave number (Glatzmaier 1985a). A dimensionless energy scale is used.

3.2. 3D convective structure

Some properties of the nonaxisymmetric components of velocity, which are responsible via nonlinear interactions for the maintenance of differential rotation, will now be examined. Simulated global convection in a rotating spherical shell tends to take the form of north-south (banana) rolls. Banana rolls develop because motions perpendicular to the axis of rotation are favored, especially at low latitude, due to the near balance that can be achieved among the pressure gradient, buoyancy, and Coriolis forces, all of which tend to be perpendicular to the axis of rotation at low latitude. The resulting small accelerations mean that this banana-roll structure is relatively stable compared to other possible convective structures. Figure 3a portrays these banana rolls with a plot of the radial component of velocity in a spherical surface just below the top boundary. Similar plots (extending 180° in longitude) from Gilman's model are illustrated in Figure 7 of Gilman & Miller (1986). This banana-roll structure has also been seen in a recent space-lab experiment of thermal convection in a rotating hemispherical shell with radial gravity (Hart, et al. 1986; Hart, Glatzmaier, & Toomre 1986; and Toomre, these proceedings).

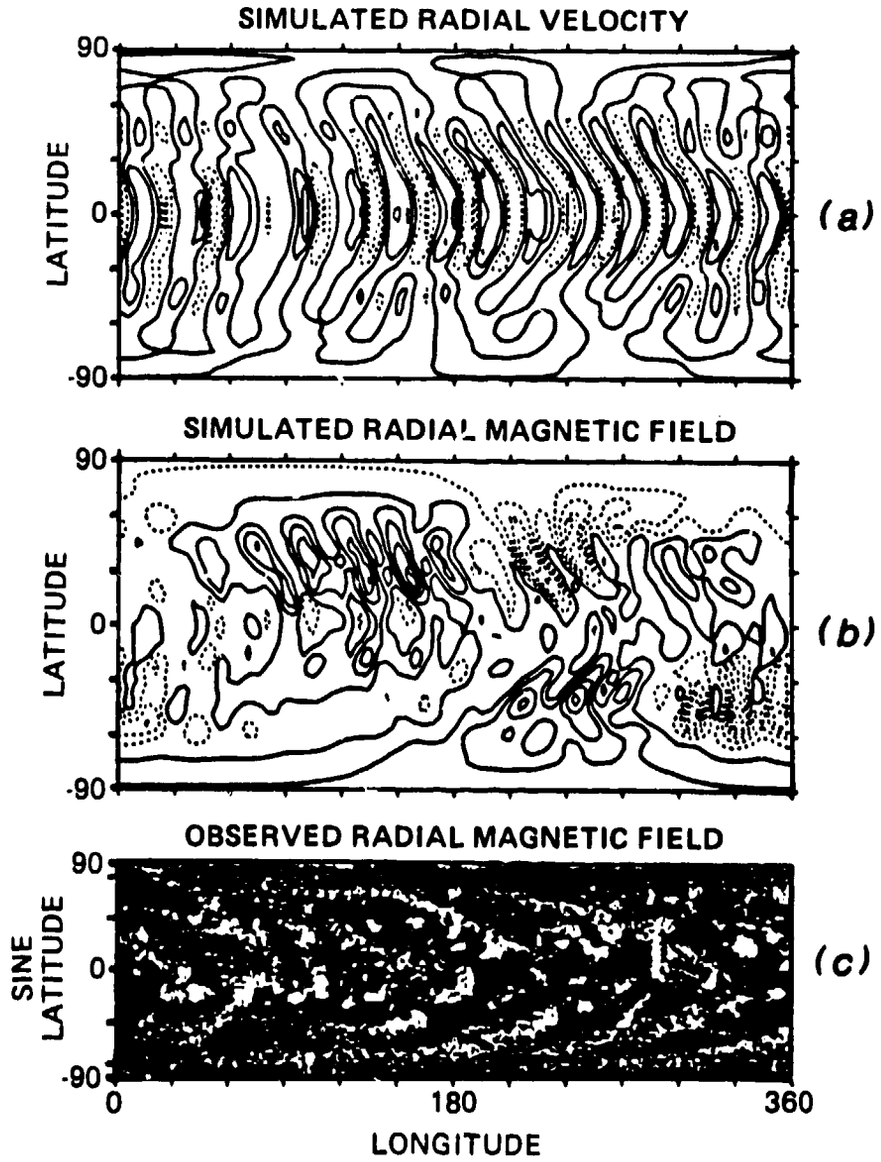

Figure 3. (a,b) Radial component of the simulated velocity and magnetic field at a given time step in a spherical surface just below the outer boundary (Glatzmaier 1984). Solid (broken) contours represent outward (inward) directed fields. (c) A Kitt Peak synoptic map of the large-scale magnetic flux at the solar surface (Carrington rotation 1705, Feb. 1981; courtesy of Dr. J. W. Harvey). Black (white) represents positive (negative) magnetic polarity.

However, there has been no direct evidence of the existence of banana rolls in the sun. If they do exist, as the numerical simulations predict, they would be very difficult to detect because the global pattern is constantly changing. Different modes propagate in longitude with different phase velocities; and these phase velocities themselves depend on latitude. This time dependence of the global pattern is easily appreciated when viewing movies of both the space-lab experiment and the numerical simulations of the experiment (Toomre, these proceedings). It can also be seen in Figure 7 of Gilman & Miller (1986) which illustrates the change during one rotation period. If long time averages are made on Doppler measurements of the solar surface velocity in order to filter out granulation and super granulation, the global convective pattern may also be filtered out. In addition, the breakup of large-scale convection into smaller horizontal scales near the surface, where the density scale-height becomes very small (Chan, these proceedings), may be responsible for the non-observance of banana rolls at the solar surface.

This later reason may also explain why a recent analysis of the movement of young sunspots (Ribes et al. 1985) suggests the existence of axisymmetric east-west rolls, not north-south banana rolls. It is possible that this is evidence of shallow meridional circulation just below the surface of the sun, above a deep banana-roll structure. It is certainly also possible that global-scale banana rolls do not exist in the sun and that the models are unsuccessful because they lack some important physical process or just do not have enough numerical resolution. These concerns will be discussed further in section 4.

However, there may be indirect evidence of banana rolls based on the measurement of large-scale solar magnetic fields. Figure 3b shows the simulated radial component of the magnetic field (in the same surface and at the same time step as in Figure 3a) generated with Glatzmaier's model running as a dynamo (Glatzmaier 1984). Notice how both polarities of the simulated magnetic field (Figure 3b) tend to be concentrated in the downdrafts of the large-scale convection (Figure 3a) where the horizontal velocity converges. This numerical simulation of the large-scale magnetic field can be compared to a Kitt Peak synoptic map of the large-scale magnetic flux at the solar surface (Figure 3c). Notice the "chevron-shaped" structure that is prominent in both the simulation and the observation. It is tempting to consider this similarity as indirect evidence of banana rolls in the deep solar convection zone.

Banana rolls are also seen in plots of the horizontal components of simulated velocity (Figure 9 of Gilman & Miller 1986). Fluid moving (relative to the rotating frame) in the direction of rotation tends to drift toward the equator and vice versa. This is due to the spherical geometry and rotation (Glatzmaier 1985a). Coriolis forces acting on the circulating fluid tend to increase or decrease the cross section of a banana roll depending on the sense of the circulation. Since the cross sections of the rolls decrease as latitude increases due to the spherical geometry, the circulating fluid drifts away from the equatorial plane if the Coriolis forces are trying to decrease the cross section of the roll. Likewise, fluid drifts toward the equatorial plane if it has the opposite sense of curculation. Therefore, as illustrated in Figure 1 of Glatzmaier (1985a), there is a net latitudinal flux of angular momentum toward the equator in both hemispheres. In addition, due to mass conservation and the density stratification, this latitudinal flux is greatest in the outer part of the convection zone where velocities are large because density is small.

As a result, angular velocity also decreases with depth. In addition, this radial differential rotation shears the nonaxisymmetric convective rolls (Gilman & Miller 1986) producing cells tilted in radius and longitude in such a way that rising fluid tends to move in the direction of rotation and sinking fluid in the opposite direction. This is illustrated in Figure 8 of Gilman & Miller (1986) and in Figure 3 of Glatzmaier (1984). Consequently, there is a net upward radial flux of angular momentum. However, this feedback process can only go so far before it finds a nonlinear equilibrium because the larger the tilt, the less

efficient the convection and therefore the smaller the convective velocities which help maintain the radial differential rotation which produces the tilt.

3.3. Meridional circulation and differential rotation

The axisymmetric part of the velocity field is divided between differential rotation, i.e., the axisymmetric longitudinal velocity relative to the rotating frame of reference, and the meridional circulation, i.e., the radial and latitudinal components of the axisymmetric velocity. The total kinetic energy in the meridional circulation is usually two orders of magnitude less than that in the differential rotation.

A typical profile of the simulated meridional circulation appears in Figure 4a. Streamlines of the mass flux illustrate how the axisymmetric flow in the equatorial region is outward in the outer part of the zone and inward in the inner part. This is mainly due to the Coriolis forces resulting from the differential rotation (Figure 5a). Note that there are also inward flows around ±50° latitude.

The outward flow at the equator causes the surface temperature to be slightly higher there; while the inward flows at ±50° latitude produce slightly lower surface temperatures (Glatzmaier 1985a). The corresponding axisymmetric part of the simulated surface temperature perturbation is illustrated in Figure 4b showing a $2K$ maximum at the equator, relative to the reference state surface temperature of $4 \times 10^5 K$, and minimums at ±50° latitude. A similar profile has been obtained for the latitudinal temperature variation on the sun using the Princeton solar distortion telescope (Kuhn et al. 1985; Kuhn, these proceedings). They see temperature minimums at ±53° latitude. The absolute temperature difference simulated is larger than that observed because the model surface is well below the photosphere. However, the ratio of the maximum temperature difference to the average temperature in that surface is somewhat less than that observed.

Finally the differential rotation, which is of major interest in these proceedings, will be discussed. In these simulations, differential rotation in latitude and radius is found to be maintained, against Coriolis and viscous forces, by the angular momentum flux which converges in the outer part of the convection zone and in the equatorial region. As described above, the angular momentum flux is a nonlinear product of nonaxisymmetric velocities which are in the form of banana rolls due to the effects of the spherical geometry, rotation, and density stratification. A typical profile of the simulated differential rotation is plotted in Figure 5a with contours of angular velocity relative to the rotating frame of reference. A similar profile, but of linear velocity, is illustrated in Figure 10 (step 18000, deep layer) of Gilman & Miller (1986). These profiles illustrate how angular velocity tends to be constant on cylinders coaxial with the rotation axis. Also plotted (Figure 5b) are the simulated latitudinal differential rotation velocities at the surface for both Gilman's and Glatzmaier's models and the solar profile obtained from Mt. Wilson Doppler measurements (Howard et al. 1983). Both models produce profiles that are in fair agreement with the observed surface differential rotation. In addition, the simulated radial differential rotation rate in the equatorial plane from Figure 5a is plotted in Figure 5c (solid curve) and compared to the rotation profile obtained from the analysis of the rotational frequency splitting of solar oscillations (dots in Figure 5c; Duvall et al. 1984; see more recent results in these proceedings). These profiles demonstrate how the simulated radial differential rotation is consistent with current observational estimates.

One point that should be emphasized is that, although the observational results show only a slight decrease (15%) in rotation rate with depth through the solar convection zone, that is all the numerical simulations have been predicting. Since the simulated profile (Figure 5a) has angular velocity constant on cylinders, the decrease of the rotation rate at the surface from the equator to about 45° latitude is essentially the same as the decrease of

the rotation rate in the equatorial plane from the surface to the base of the convection zone. The differential rotation portrayed in Figure 5a appears very substantial because it plotted relative to the rotating frame of reference. However, the absolute variation in radius simulated by the models and plotted in Figure 5c is actually only about 15% of the surface rotation rate.

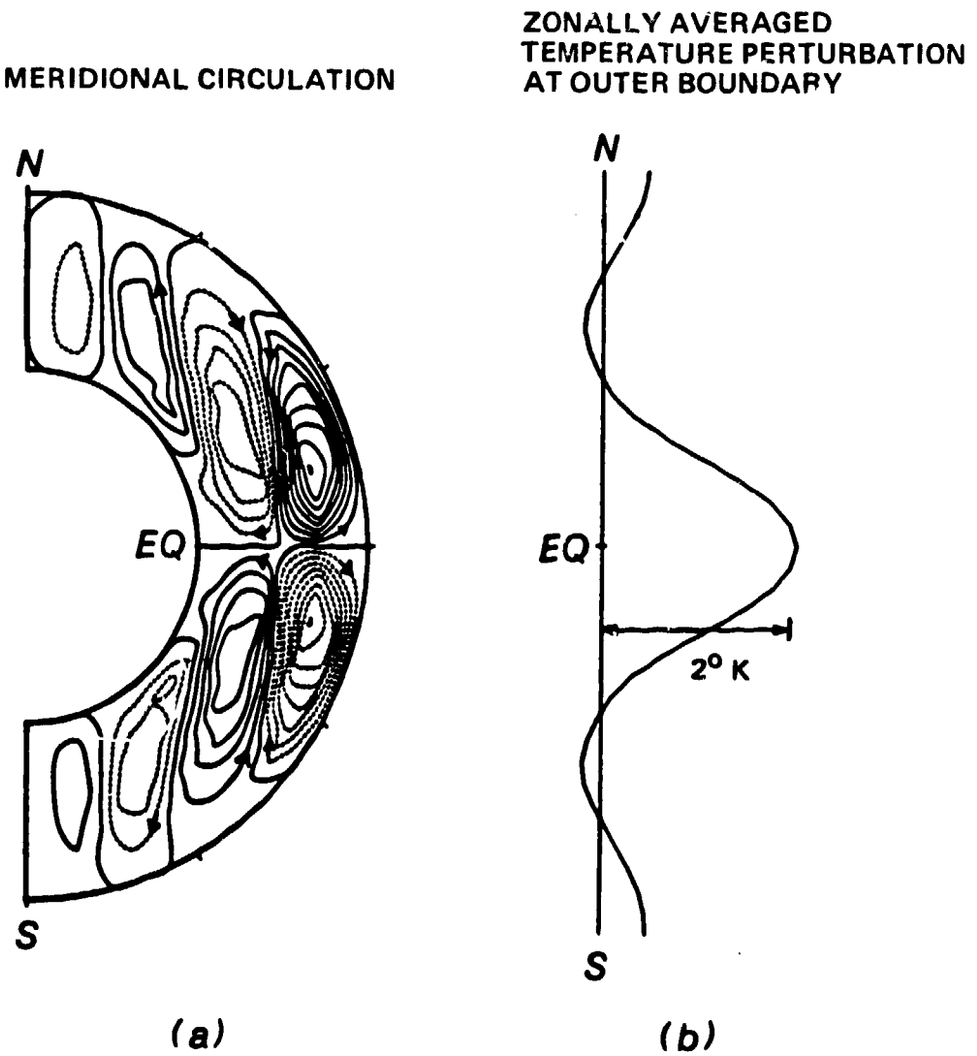

Figure 4. (a) Streamlines of the axisymmetric mass flux plotted in a meridian plane. (b) The latitudinal variation of the axisymmetric temperature perturbation at the outer boundary (93% of solar radius) relative to the reference state boundary temperature of 4×10^5K (Glatzmaier 1985a).

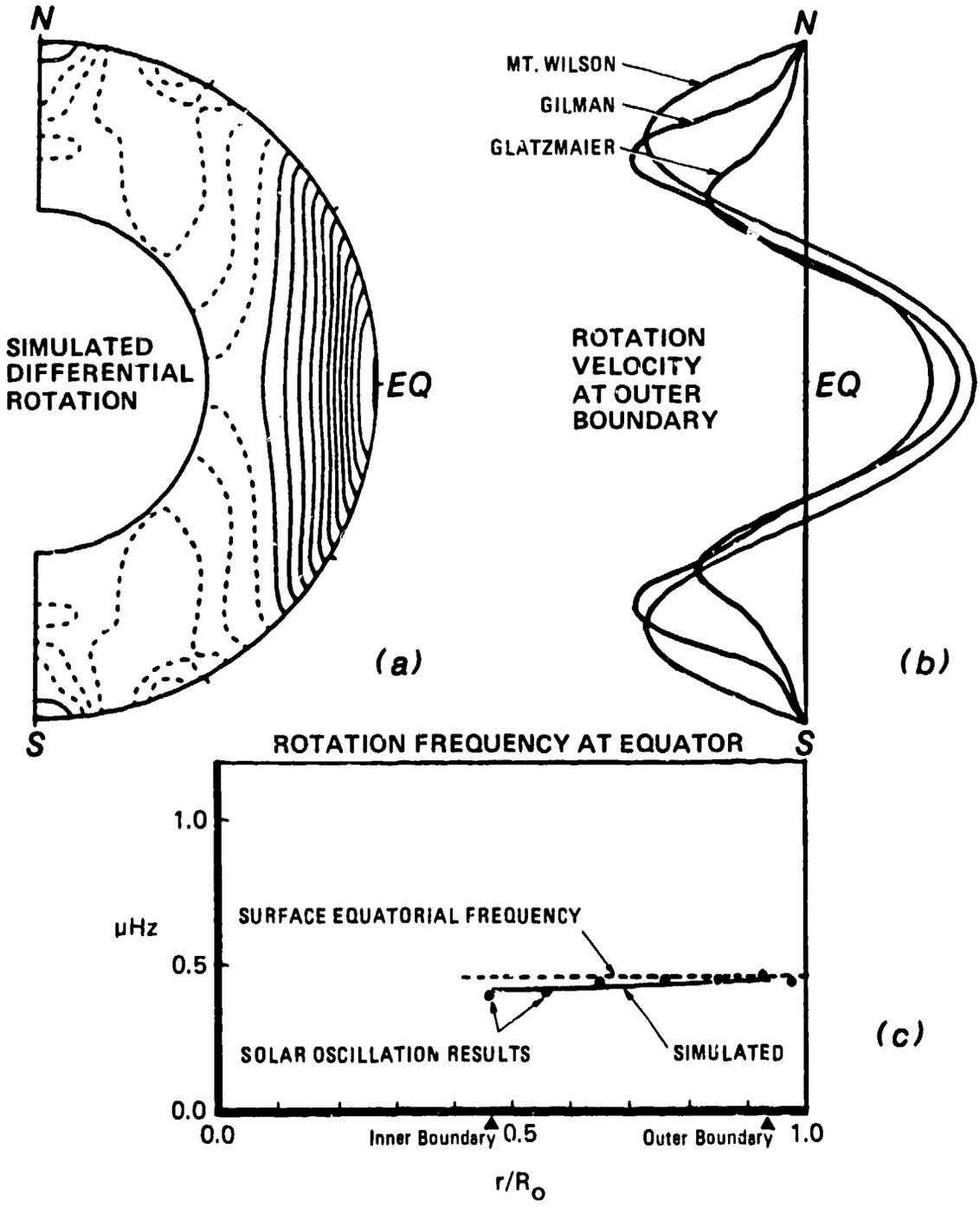

Figure 5. (a) Simulated angular velocity relative to the rotating frame of reference (Glatzmaier 1985a). (b) Simulated surface rotation velocity (Gilman & Miller 1986; Glatzmaier 1985a) and observed solar surface rotation velocity at Mt. Wilson (Howard et al. 1983). (c) Simulated angular velocity as a function of radius (solid curve, Glatzmaier 1985a) and estimates from the analysis of the frequency splitting of solar oscillations (dots, Duvall et al. 1984).

4. DISCUSSION OF VALIDITY

Having briefly described the three-dimensional models and compared their solutions to solar observations, an important question arises. How well do these numerical solutions represent the actual physical processes in the sun? Actually, this question should be broken into two. Do the codes accurately solve the model equations and do the model equations adequately describe the solar physics?

4.1. Do the codes accurately solve the model equations?

Although there will always be some degree of error in these numerical solutions due to numerical truncation and limited numerical resolution in space and time, it is hoped that enough accuracy is achieved that certainly the qualitative features and, to a good extent, the quantitative features do not depend on the particular details of the numerical solution technique. Fortunately, this has been the case for the two models described here. These models, being developed completely independently and employing very different numerical techniques, have produced essentially the same numerical solutions. Solutions to a nonlinear system of equations that describe how the three components of velocity and three thermodynamic variables are updated every time step on well over 50,000 grid points for tens of thousands of time steps. The probability is quite small that both of these two very different numerical codes are generating erroneous solutions that agree so well with each other. This is indirect evidence that the codes are accurately solving the model equations.

Direct evidence now also exists. Very good qualitative agreement has been found between a recent space-lab experiment of thermal convection in a rotating hemispherical shell and the three-dimensional numerical simulations of it done with a modified version of Glatzmaier's code (Hart et al. 1986; Hart, Glatzmaier, & Toomre 1986; Toomre, these proceedings). Different scenarios, defined by the temperature boundary conditions, the strength of the central gravity, and the rotation rate, produced quite different convective structures including banana rolls, spirals, "soccer ball" patterns, and triangular waves. In all cases that could adequately be resolved numerically, the model produced numerical solutions in agreement with the experiment without any tuning or model adjustments whatsoever. However, one must realize that the convecting fluid in this experiment was a liquid, not a stratified gas like the sun. Also, the actual molecular diffusivities of the liquid were use in the model, not parameterized eddy diffusivities as are required for simulations of the sun. Yet this demonstrated agreement is direct evidence that the computer code is accurately solving the three-dimensional nonlinear system of equations that describes this thermal convection experiment.

4.2. Do the model equations adequately describe the solar physics?

The answer to this question is not so obvious. There are several concerns stemming from the limitations of three-dimensional numerical simulations.

There is concern about the inner and outer impermeable spherical boundaries that are imposed in both models. The inner boundary could be removed by solving the equations everywhere in a full sphere. This poses additional numerical complications, but not difficult ones. This would also allow the three-dimensional simulation of gravity waves in the radiative solar interior and the theoretical investigation of differential rotation in the center of the sun. The outer boundary, as mentioned above, is not placed at the photosphere, but rather 5% to 10% of the solar radius below the photosphere in order of avoid the large additional number of grid points that would be required to adequately

resolve this region of small scale-heights. Consequently, it is possible that the models neglect some very important physical processes near the solar surface.

Another concern is the depth of the convection zone which is specified in these models. Both models have demonstrated that the deeper the convection zone, the better the resulting surface differential rotation profile matches the observed solar profile and the less tendency for a polar vortex which has not been observed. On the other hand, the solar abundances of lithium and beryllium place a limit on the depth of the solar convection zone.

However, the major concern about these models is the parameterized eddy diffusivities which are treated as scalar quantities. As mentioned above, these diffusivities are either specified time-independent functions of radius or time-dependent functions of the local shear of the large-scale resolved velocity fields. Several more sophisticated parameterizations should be tested. For example, diffusion in the radial direction probably should be a function of the local Richardson number which accounts for both local stability (radial entropy gradient) and local wind shear. Also, accounting for Coriolis forces on the subgrid-scale eddies via a tensor formulation like that suggested by Durney (these proceedings) may introduce new effects.

The effects of different specified scalar diffusivities have been investigated to some extent with the three-dimensional models. Both models have demonstrated that the more the diffusivities vary in radius the less solar-like the surface differential rotation. Also, as the viscous and thermal diffusivities decrease, for a given spatial resolution, differential rotation kinetic energy increases faster than convection kinetic energy. If the ratio of viscous to thermal diffusivity decreases, the ratio of differential rotation kinetic energy to meridional kinetic energy increases. However, it should be pointed out that, although the models can produce an angular velocity increasing with depth (with a special combination of eddy diffusivities and convection zone depth), the latitudinal differential rotation at the surface in these cases looks nothing like the sun's. Whenever a solar-like surface differential rotation is obtained, the simulated angular velocity decreases with depth as illustrated in Figure 5.

One way to deal with the problem of ad hoc eddy diffusivity parameterizations is to increase the spatial and temporal resolution of the model in order to resolve more scales and decrease the amplitude, effect, and significance of the eddy diffusivities which parameterize the effects of the unresolved scales. That is, increase the role of physics in the numerical simulation while decreasing the role of parameterization. Of course the limitations of computers will always limit numerical resolution.

On the other hand, as seen in Figure 14 of Gilman & Miller (1986), most of the nonlinear work to maintain the simulated differential rotation is done by resolved modes with longitudinal wave numbers between 8 and 20. Therefore, whereas an increase in spatial resolution would provide better information about the small scales, it probably would not significantly change the large-scale structure of the simulated differential rotation.

Although a banana-roll structure has not been observed at the solar surface, the fact that the numerical simulations from both models are in fair agreement with several other solar observations provides some confidence that the physics pertaining to deep global convection is adequately described by the equations. As discussed above, the surface structure of the large-scale magnetic flux simulated by the model when in a dynamo mode is quite similar to that seen in Kitt Peak magnetic synoptic maps. (However, problems still exist with magnetic cycle simulations (Gilman 1983; Glatzmaier 1985a,b).) The surface temperature variation with latitude is in fair agreement with observations made with the Princeton solar distortion telescope. The latitudinal differential rotation at the surface is also in fair agreement with Mt. Wilson Doppler measurements. The radial differential

rotation through the convection zone is consistent with the analysis of the rotational frequency splitting of solar oscillations. These observations have been explained with relatively simple physical arguments once the numerical models demonstrated, within the limitations described above, that these arguments are consistent with the global, three-dimensional, nonlinear equations that describe mass, momentum, and energy conservation.

ACKNOWLEDGMENT

I would like to thank Dr. Peter Gilman for helpful discussions concerning this review.

REFERENCES

Duvall, T.L., Dziembowski, W.A., Goode, P.R., Gough, D.O., Harvey, J.W. and Leibacher, J.W. 1984, *Nature*, **310**, 22.
Gilman, P.A. 1977, *Geophys. Ap. Fluid Dyn.*, **8**, 93.
_____. 1983, *Ap. J. Suppl.*, **53**, 243.
Gilman, P.A. and Glatzamier, G.A. 1981, *Ap. J. Suppl.*, **45**, 335.
Gilman, P.A. and Miller, J. 1981, *Ap. J. Suppl.*, **46**, 211.
_____. 1986, *Ap. J. Suppl.*, **61**, 585.
Glatzmaier, G.A. 1984, *J. Comp. Phys.*, **55**, 461.
_____. 1985a, *Ap. J.*, **291**, 300.
_____. 1985b, *Geophys. Ap. Fluid Dyn.*, **31**, 137.
Gough, D.O. 1969, *J. Atmos. Sci.*, **26**, 448.
Hart, J.E., Glatzmaier, G.A. and Toomre, J. 1986, *J. Fluid Mech.*, (in press).
Hart, J.E., Toomre, J., Deane, A.E., Hurlburt, N.E., Glatzmaier, G.A., Fichtl, G.H., Leslie, F., Fowlis, W.W. and Gilman, P.A. 1986, *Science*, **234**, 61.
Howard, R., Adkins, J.M., Boyden, J.E., Cragg, T.A., Gregory, T.S., LaBonte, B.J., Padilla, S.P. and Webster, L. 1983, *Solar Physics*, **83**, 321.
Kuhn, J.R., Libbrech, K.G. and Dicke, R.H. 1985, *Ap. J.*, **290**, 758.
Ribes, E., Mein, P. and Mangeney, A. 1985, *Nature*, **318**, 170.